Progress in Fractional Differentiation and Applications
An International Journal

http://dx.doi.org/10.18576/pfda/080303

Tuning of the Fractional-order PID Controller for some Real-life Industrial Processes Using Particle Swarm Optimization

Shaher Momani[1,2,*] *and Iqbal M. Batiha*[2,3]

[1] Department of Mathematics, Faculty of Science, The University of Jordan, Amman 11942, Jordan
[2] Nonlinear Dynamics Research Center (NDRC), Ajman University, Ajman 346, UAE
[3] Department of Mathematics, Faculty of Science and Technology, Irbid National University, Irbid 2600, Jordan

Received: 16 Nov. 2021, Revised: 18 Dec. 2021, Accepted: 21 Jan. 2022
Published online: 1 Jul. 2022

Abstract: In this paper, several feedback control methods are proposed for some real-life industrial processes. All these methods are designed to obtain an optimal tuning for the Fractional-order PID controller using two optimization techniques; Particle Swarm Optimization (PSO) and Bacteria Foraging Optimization (BFO). Such methods have been inferred by including several approaches for the fractional-order integro-differential Laplacian operators within the PSO and BFO algorithms. These approaches are: The Continued Fractional Expansion (CFE) approach, Oustaloup's approach, the 1^{st}- and the 2^{nd}-order El-Khazali's approaches. Different forms of integer-order rational transfer functions for such operators have been deduced corresponding to these approaches, which allow one to develop realizable models for some industrial applications. Numerous numerical simulations of the dynamic responses are explored and discussed for the purpose of illustrating the influence and the efficiency of all designed methods.

Keywords: $PI^{\lambda}D^{\delta}$-controller, particle swarm optimization algorithm, bacteria foraging optimization, Laplacian operator, Oustaloup's approach, continued fractional expansion approach, El-Khazali's approaches.

1 Introduction

Over the past few decades, the fractional-order dynamic systems (FoDSs) together with their proposed controllers have been extensively explored within different fields associated with applied science and engineering [1]. To meet the great advance in modern control theories, several types of controllers have been and still being proposed; such as fuzzy-, neural network-, predictive-, unified feedback-, and optimal-controllers [2]. The proportional–integral–derivative controller (or simply PID-controller), which is one of the most significant controllers, is still being widely employed nowadays in a large number of industrial processes. Actually, upwards of 90% of these processes are performed based on such controller [2]. The reason for this utilization is referred to some useful proprieties that this controller has. Furthermore, it has been shown that this controller has a very simple construction, which allows engineers to easily understand its form. It, furthermore, has a powerful performance to achieve a better change to the whole of the industrial process. In addition, it has been declared that this controller is indeed simple to design and easy to implement within several real-time applications [2]. However, although all these features are inherent in this controller, it has been recently shown that it does not offer an optimum adjustment for the controlled system because it generates a large overshoot in the response of the system. This matter has increasingly motivated a lot of researchers to seek executable solutions for the purpose of improving the performance of such controller. The main one of those granulomatous solutions have been established based on employing the conception of fractional calculus, which handles the derivative, as well as the integral in its fractional-order form instead of its integer-order one. The idea of this solution was based on proposing a modified controller of the PID-controller itself which is called the Fractional-order PID controller (or simply $PI^{\lambda}D^{\delta}$-controller) [2,3,4]. This controller

* Corresponding author e-mail: s.momani@ajman.ac.ae

shows its superior robustness, outstanding performance, and high flexibility in comparison with the classical one. One of the main reasons that makes this controller possesses such characteristics is the fractional-order of its differentiation and integration operators that provides more degrees of freedom in system designing [5]. Notwithstanding all these features for this controller, it faces a significant task, which has become a focal point for many researchers, represented by the optimal tuning of its parameters that should be undoubtedly handled [6]. In particular, this controller has five parameters that should be tuned in order to satisfy some needed features for the system. These parameters are the three constant gains (K_p, K_i, K_d) for the proportional, integral and derivative terms, together with the fractional-order values of the integration and differentiation operators (λ) and (δ), respectively [2].

Recently, many swarm intelligence algorithms have been widely developed for the purpose of facing immense number of complicated optimization problems. Due to the fact that finding the parameters of the $PI^{\lambda}D^{\delta}$-controller is just one of these problems, several optimization algorithms have been employed for tuning these parameters. Among all of such algorithms, the Particle Swarm Optimization (PSO) and the Bacteria Foraging Optimization (BFO) algorithms have made their mark and demonstrated their potency in this field [7]. The PSO algorithm, which was first proposed by Kennedy and Eberhart in 1995 [8,9], enjoys simple procedures, efficient computations and easiness implementation [5,9]. On the other hand, the BFO algorithm, which was proposed in 2002 by Passino [10], is a new arrival algorithm to the class of optimization techniques, which characterized by a graceful structure and a biological motivation as reported [7]. In general, the PSO and BFO algorithms have been successfully carried out in several industrial applications such as machine learning, transmission loss reduction, harmonic estimation, optimal control engineering, and many more (see [11,12,13] and references therein). However, in this work, these two algorithms will be implemented to find optimal values of the five parameters of the $PI^{\lambda}D^{\delta}$-controller in order to meet high performance for some electric motor drives. More precisely, the main target of such optimizations is to minimize the value of the fitness function in view of some constraints associated with time or frequency domain, such as maximum settling time, rise time and overshoot, or subject to the gain and phase margins of the system. Actually, these constraints play a key role in measuring the robustness of the system under control [14,15]. It is quite natural that, after the successful of the optimization algorithms in obtaining the optimum values of the $PI^{\lambda}D^{\delta}$-controller, attention would be directed toward the other major next task, which concerns with dealing with the fractional-order Laplacian operator s^{λ} and/or s^{δ} (or simply $s^{\pm\alpha}$, where $\alpha = \{\lambda,\ \delta\}$), $0 < \alpha < 1$. As a result of the arbitrariness of this operator, its analytical form could be only granted as a finite-order rational transfer functions enabling one to analyze and design the controlled system without required handling of some tough time-domain formulations [14,15]. These transfer functions, which are convenient to use and their features are quite close to the original system features, could be generated using several methods and approaches such as the Continued Fraction Expansion (CFE) [16], Matsuda's [17], Carlson's [18], and Oustaloup's [16,17,19] approaches.

Recently, El-Khazali introduced his 1^{st}- and 2^{nd}-approaches in [20] and [21], respectively, for approximating $s^{\pm\alpha}$, where $0 < \alpha < 1$. It has been shown that such two approaches may have significant influence on the required optimum results (see [14,15]). Besides, the use of these methods will, fortunately, reduce the order of the system more than any other approaches. Therefore, from the perspective of the benefits of these two approaches, they will be next carried out together with two other approaches, the CFE and Oustaloup's approaches, to provide $s^{\pm\alpha}$ with its corresponding rational transfer functions. As far as we know, designing new $PI^{\lambda}D^{\delta}$-controllers for some electric motor drives systems using the PSO and BFO algorithms via four approaches to $s^{\pm\alpha}$ remains, up to this day, mostly unexplored topic. For simplicity, these optimal controllers will be denoted by the $PI^{\lambda}D^{\delta}$-PSO/BFO via CFE approach, $PI^{\lambda}D^{\delta}$-PSO/BFO via Oustaloup's approach, $PI^{\lambda}D^{\delta}$-PSO/BFO via 1^{st}-order El-Khazali's approach, and $PI^{\lambda}D^{\delta}$-PSO/BFO via 2^{nd}-order El-Khazali's approach. In addition, all these eight controllers will be compared in accordance with their performances in providing some handled systems with best dynamic response characteristics, such as providing the minimal overshoot percentage, least rise time and least settling time.

This paper will be organized as follows: The following next section introduces the concept of the fractional-order linear time-invariant system, followed by some preliminaries associated with the fractional-order PID controllers which are briefly presented in Section 3. Some finite-order rational approaches of the fractional-order integro-differential Laplacian operators are described in Section 4, while the last section exhibits all numerical findings resulted from applying the proposed schemes on two industrial applications, namely the linear Brushless (BLDC) DC motor and the Servo DC motor.

2 Fractional-order linear time-invariant systems

Generally, the primary concepts of fractional calculus are employed to turn the so-called integer-order Linear Time-Invariant (LTI) systems into their fractional-order cases to be next named the Fractional-order LTI systems (or simply FoLTI systems) [3,22]. It is common knowledge that such systems are exact generalizations of those integer-order ones. In view of some evidences reported [3,23], it was demonstrated that these FoLTI systems surpass the other classical counterparts because of their flexibility in considering further parameters. However, the following fractional-order differential equation represents the considered FoLTI systems in this work [3]:

$$z_n D^{\rho_n} y(t) + \ldots + z_0 D^{\rho_0} y(t) = w_m D^{\nu_m} u(t) + \ldots + w_0 D^{\nu_0} u(t) \tag{1}$$

where $y(t)$ and $u(t)$ are two variables over the time t that indicate to the control output and input of the system respectively, and where $D^{\{\rho_i,\nu_k\}}$ represents the Caputo operator of orders $\rho_i; i = 1,2,3,\ldots,n$, and $\nu_k; k = 1,2,3,\ldots,m$, such that $n,m \in \mathbb{N}$.

As a matter of fact, system (1) mathematically matches the LTI filter of infinite dimension. For the purpose of modeling this system, one should realize its form as a finite-order rational transfer function, which will enable one to analyze and design the controlled system without required handling of some tough time-domain formulations. In fact, the high/low degree of these approximate transfer functions relies on the numerical method that generated them. In the same framework, such transfer function plays a key role in representing the frequency response of LTI filters. In particular, the transfer function of any of these filters can be represented by the ratio between two Laplace transforms of both system's output and input in accordance with zero initial conditions [24]. In other words, the transfer function that represents the standard form of the FoLTI system given in (1) can be expressed as follows [24,25]:

$$G(s) = \frac{Y(s)}{U(s)} = \frac{w_m s^{\nu_m} + w_{m-1} s^{\nu_{m-1}} + \ldots + w_1 s^{\nu_1} + w_0 s^{\nu_0}}{z_n s^{\rho_n} + z_{n-1} s^{\rho_{n-1}} + \ldots + z_1 s^{\rho_1} + z_0 s^{\rho_0}}, \tag{2}$$

where $Y(s) = \mathscr{L}\{y(t)\}$, $U(s) = \mathscr{L}\{u(t)\}$ are the Laplace transforms of $y(t)$ and $u(t)$, respectively.

3 Fractional-order PID controllers

In 1997, Podlubny et al. proposed the main construction of the $PI^{\lambda}D^{\delta}$-controller in [26]. They evidently demonstrated its advantages in providing more rapid response and better performance than the classical PID-controller. From this point of view, several real-life industrial processes and applications are currently employing this controller. Actually, its construction is based on adding two extra parameters (λ and δ) to the main parameters, (K_p, K_i, K_d), of the PID-controller. These two parameters, which respectively represent the fractional integral and differential operators, offer further degree of freedom within tuning algorithms. However, the $PI^{\lambda}D^{\delta}$-controller is certainly deduced from the following integro-differential equation [3,26]:

$$u(t) = K_p e(t) + K_i J^{\lambda} e(t) + K_d D^{\delta} e(t), \tag{3}$$

where D^{δ} is the Caputo operator of order δ, J^{λ} is the Riemann-Liouville operator of order λ, and $e(t)$ is the error signal. Taking the Laplace transform of (3) yields exactly the final version of the $PI^{\lambda}D^{\delta}$-controller, which would be of the following form:

$$C(s) = \frac{U(s)}{E(s)} = K_p + K_i s^{-\lambda} + K_d s^{\delta}. \tag{4}$$

where $E(s) = \mathscr{L}\{e(t)\}$ is the Laplace transforms of $e(t)$.

The next task focuses on taking the $PI^{\lambda}D^{\delta}$-controller along with two industrial systems for the purpose of improving their process control. This involves carrying out a certain optimization algorithm trying to improve the unit-step response of the system through optimal tuning the five parameters of the $PI^{\lambda}D^{\delta}$-controller. In this work, the PSO and BFO algorithms will be implemented to find the optimum values of those parameters via several approaches for the operators $s^{\pm\alpha}$ shown in (4), where $\alpha = \{\lambda,\ \delta\}$, $0 < \alpha < 1$. From the perspective of the whole scheme, there is definitely an optimization problem, which made it necessary to set up the so called fitness function within these algorithms. In view of this fact, there are several common fitness functions that might be employed for designing the best points of the $PI^{\lambda}D^{\delta}$-controller, such as Integral Time Square Error (ITSE), Integral Square Error (ISE), Integral Absolute Error (IAE) and Integral Time-Absolute Error (ITAE). In particular, minimizing the value of any fitness function is the main target of the considered optimization algorithm for the purpose of attaining the optimum values of the $PI^{\lambda}D^{\delta}$-controller. For more details about these two algorithms and how some fitness functions look like within, the reader may refer to the references [5,7,9,27,28,29]. However, the overall tuning process of the $PI^{\lambda}D^{\delta}$-controller's parameters using PSO and BFO algorithms could be described by the block diagram shown in Figure 1.

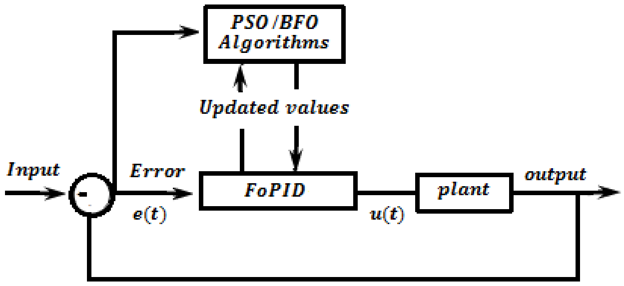

Fig. 1: Block diagram of PSO/BFO running to tune the $PI^{\lambda}D^{\delta}$-controller

In addition to the role of the fitness functions in tuning the optimum parameters of the $PI^{\lambda}D^{\delta}$-controller, this work utilizes one that depends on metering the main criteria associated with the time domain. More precisely, the fitness function, which will be considered in this work, consists of four aspects; the steady-state error, settling time, rise time, and peak overshoot [6,9]. However, the following is how the fitness function can be expressed [6,9]:

$$J=(1-e^{\beta})(M_p+E_{ss})+e^{-\beta}(T_s-T_r), \tag{5}$$

where β is the scaling factor, M_p is the peak overshoot, E_{ss} is the steady state error, T_s is the settling time, and T_r is the rise time.

It is worth noting that the scaling factor β, which typically relies on a designer's choice, certainly determines the contribution of the four mentioned aspects towards the primary fitness function [6,9]. In particular, we chose this factor here to be equal 0.5, based on the assertion that when β is greater than 0.7, the steady states error and overshoot will be further reduced, and when it is smaller than 0.7, the rise time and settling time will be further reduced [9].

4 Rational approaches of fractional-order operators

In this section, four finite-order rational approaches of the fractional-order integro-differential Laplacian operators, $s^{\pm\alpha}$ are taken into account, where $0<\alpha<1$. These approaches are: The 1^{st}-order El-Khazali's approach which has been well defined in [20], the 2^{nd}-order El-Khazali's approach which has been broadly outlined in [16,21,23,25], Oustaloup's approach that were extensively employed in many references [25,30], and finally the CFE approach which is the only approach that will be briefly described in this work for completeness.

4.1 The CFE approach

This method is deemed the primary mathematical approach for providing the operators $s^{\pm\alpha}$ by proper rational transfer functions. Such approach had been established based on the following approximation [31]:

$$(1+z)^{\alpha}=\cfrac{1}{1-\cfrac{\alpha z}{1+\cfrac{(1+\alpha)z}{2+\cfrac{(1-\alpha)z}{3-\cfrac{(2+\alpha)z}{2+\cfrac{(2-\alpha)z}{5+\cfrac{\ldots+(n+\alpha)z}{2+\cfrac{(n-\alpha)z}{2n+1+\ldots}}}}}}}}, \tag{6}$$

where, $0<\alpha<1$ and $n\in\mathbb{N}$. For simplicity, the form in (6) can be expressed in the following equivalent form [27]:

$$(1+z)^{\alpha}=\frac{1}{1-}\,\frac{\alpha z}{1+}\,\frac{(1+\alpha)z}{2+}\,\frac{(1-\alpha)z}{3+}\,\frac{(2+\alpha)z}{2+}\,\frac{(2-\alpha)z}{5+}\,\frac{(n+\alpha)z}{2+}\,\frac{(n-\alpha)z}{2n+1+}. \tag{7}$$

For the purpose of obtaining a finite-order approximation of the operator s^{α}, one might replace the term $s-1$ instead of the variable z in (7). This exchange step enables the n^{th}-order approximation of such operator to be appeared around the center frequency $\omega_0=1\,rad/sec$ as follows [31]:

$$s^{\alpha}\cong\frac{\alpha_0 s^n+\alpha_1 s^{n-1}+\ldots+\alpha_{n-1}s+\alpha_n}{\alpha_n s^n+\alpha_{n-1}s^{n-1}+\ldots+\alpha_1 s+\alpha_0}, \tag{8}$$

where $0 < \alpha_i < 1$, $i = 0,1,,2,\ldots,5$. In particular, the coefficients' values of α_i can be found, for $i = 0,1,...,5$. Besides, the operator $s^{-\alpha}$ can be simply obtained by inverting upside down the expression given in (18).

In general, the need to use the previously stated approaches arise immediately after obtaining the optimum values of the $PI^{\lambda}D^{\delta}$-controller through some optimization algorithms. These four approaches, which will be just finite-order rational transfer functions, allow one to analyze and design the controlled system without required handling some tough time-domain formulations [14,15]. To highlight the major similarities between these approaches, two comparisons have been made between all rational transfer functions for approximating the operator $s^{0.5}$ in view of the time and frequency responses. In particular, the step responses and the bode diagrams of the following approximations are exhibited in Figures 2 and 3, respectively.

– The 1^{st}-El-Khazali's approach:

$$s^{0.5} = \frac{2.414s+1}{s+2.414}. \tag{9}$$

– The 2^{nd}-El-Khazali's approach:

$$s^{0.5} = \frac{2.707s^2+4.828s+0.7071}{0.7071s^2+4.828s+2.707}. \tag{10}$$

– Oustaloup's approach:

$$s^{0.5} = \frac{10s^5+298.5s^4+1218s^3+768.5s^2+74.97s+1}{s^5+74.97s^4+768.5s^3+1218s^2+298.5s+10}. \tag{11}$$

– The CFE approach:

$$s^{0.5} = \frac{11s^5+165s^4+462s^3+330s^2+55s+1}{s^5+55s^4+330s^3+462s^2+165s+11}. \tag{12}$$

In view of Figure 2, one might easily observed that all step responses of the operator $s^{0.5}$ using the four approximations given by (9)–(12), besides all the frequency responses shown in Figure 3, are almost identical responses.

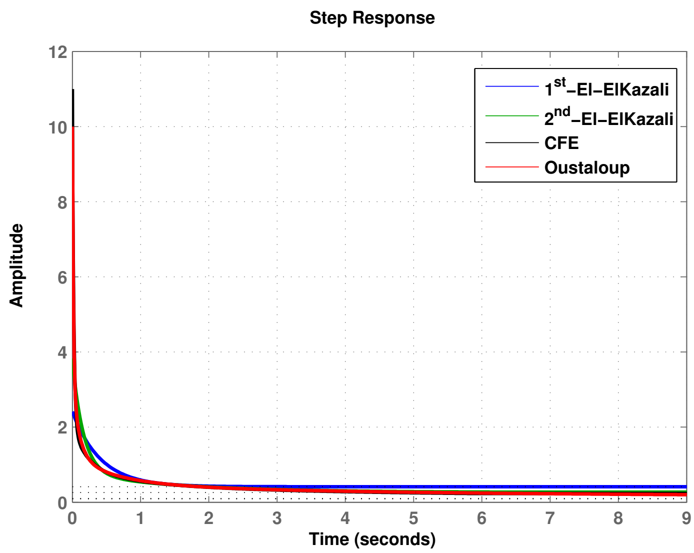

Fig. 2: Step responses of $s^{0.5}$ using (9)–(12).

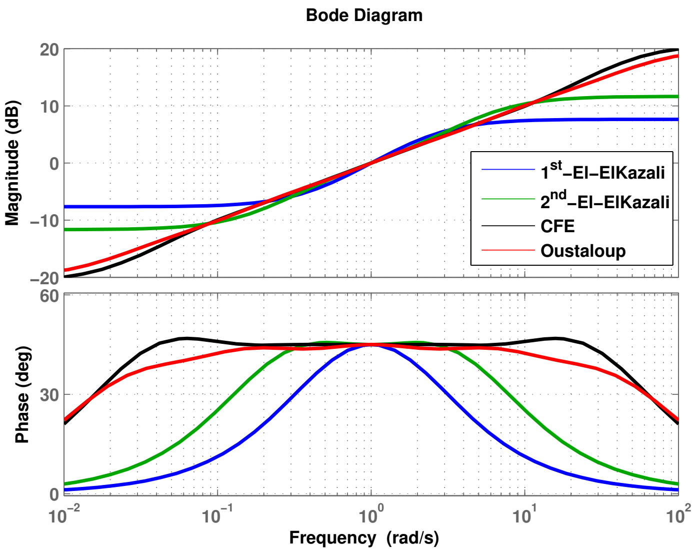

Fig. 3: Bode diagrams of $s^{0.5}$ using (9)–(12).

5 Some industrial applications

From the principle of the extreme importance of electric motors in lots of industrial applications comes the need to frequently pay attention to improve their performance as possible. Such motors can be found everywhere around us; in our cars, fans, dryers, washers, pumps, air conditioners, refrigerators, etc. The speed of those motors is inversely proportional to the flux of the magnetic field, and directly proportional to the armature voltage [32]. Thus, controlling of the field current and/or the armature voltage will adjust their speed [32]. For this purpose, lots of controllers, including the $PI^{\lambda}D^{\delta}$-controller, have been employed in order to carry out this controlling task. Actually, the $PI^{\lambda}D^{\delta}$-controller provides an effective solution to several real-life control issues [9]. In this section, several $PI^{\lambda}D^{\delta}$-controllers in accordance with two mainly types of electric motors, namely the Brushless DC motor (or simply BLDC motor) and the Servo DC motor, will be designed in order to obtain better dynamic responses of their systems which in turn provide high performance for these motors. Of course, all these design methods will be implemented through employing the PSO and BFO algorithms with considering all aforesaid approaches of the operators $s^{\pm\alpha}$. Actually, it would be eight feedback design methods after considering these two algorithms together with the four approaches of $s^{\pm\alpha}$. These methods are $PI^{\lambda}D^{\delta}$-PSO/BFO via CFE approach, $PI^{\lambda}D^{\delta}$-PSO/BFO via Oustaloup's approach, $PI^{\lambda}D^{\delta}$-PSO/BFO via 1^{st}-order El-Khazali's approach, and $PI^{\lambda}D^{\delta}$-PSO/BFO via 2^{nd}-order El-Khazali's approach. However, the following two subsections focus on describing the tune process of the $PI^{\lambda}D^{\delta}$-controller for BLDC and Servo DC motors, respectively.

5.1 Design of $PI^{\lambda}D^{\delta}$-controller for a linear BLDC motor

In recent time, several novel control strategies have been broadly established to enhance the performance of BLDC motor, (see [9] and references therein). In [25], a special case of the BLDC motor system has been recently handled through considering the coefficient of s consists of only one term in the denominator part via just using the 2^{nd}-order El-Khazali's approach. However, in this part, we intend to design several optimal $PI^{\lambda}D^{\delta}$-controllers for speed control of a linear BLDC motor rather than that previously proposed. For this purpose, we refer to the transfer function of the motor speed $w(t)$ to the armature voltage $v(t)$ reported in [9,32] as follows:

$$G(s)=\frac{W(s)}{V(s)}=\frac{K_t}{JLs^2+(DL+JR)s+K_tK_b}, \tag{13}$$

where $W(s)=\mathscr{L}\{w(t)\}$ and $V(s)=\mathscr{L}\{v(t)\}$ are respectively the Laplace transforms of $w(t)$ and $v(t)$, and where K_t is the motor torque constant, J is the moment of inertia, L is the inductance of the stator, D is the viscous coefficient, R is the resistance of the stator, and K_b is the back electromotive force constant. In view of the parameters' values given in [9], one can obtained the following transfer function:

$$G(s)=\frac{0.1433}{0.052\times10^{-5}s^2+0.0002172s+0.02053489}. \tag{14}$$

To demonstrate all feedback design methods of the $PI^{\lambda}D^{\delta}$-controllers, let us minimize, as much as possible, the value of the fitness function given in (5) by executing the PSO and BFO algorithms that consider the four approaches of the operators $s^{\pm\alpha}$ mentioned in Section 4. The maximum number of iterations and the population size, within both two algorithms, have been assumed 100 and 20, respectively. However, in order to obtain a clear view, we have arranged the overall results of these optimizations by stating firstly the $PI^{\lambda}D^{\delta}$-controller $C(s)$, secondly the same controller but via a certain approach, and finally the closed-loop of the system $H(s)$ according to each controller.

–The $PI^{\lambda}D^{\delta}$-PSO controller via 1^{st}-order El-Khazali's approach:

$$C(s) = 29.1798 + \frac{1}{s^{0.862}} + 52s^{0.987}, \tag{15}$$

$$C_{\{1^{st}-Kh\}}(s) = \frac{4.707e004s^2 + 3.197e004s + 3810}{9.19s^2 + 901.1s + 97.94}, \tag{16}$$

$$H^{PSO}_{\{1^{st}-Kh\}}(s) = \frac{6746s^2 + 4581s + 546}{4.779e-006s^4 + 0.002465s^3 + 6746s^2 + 4600s + 548}. \tag{17}$$

–The $PI^{\lambda}D^{\delta}$-PSO controller via 2^{nd}-order El-Khazali's approach:

$$C(s) = 1 + \frac{1}{s^{0.928}} + 54s^{0.305382}, \tag{18}$$

$$C_{\{2^{nd}-Kh\}}(s) = \frac{476.2s^4 + 1568s^3 + 1408s^2 + 302.8s + 13.43}{4.111s^4 + 23.44s^3 + 29.59s^2 + 9.975s + 0.1777}, \tag{19}$$

$$H^{PSO}_{\{2^{nd}-Kh\}}(s) = \frac{68.24s^4 + 224.7s^3 + 201.7s^2 + 43.39s + 1.925}{2.138e-006s^6 + 0.0009051s^5 + 68.33s^4 + 225.2s^3 + 202.3s^2 + 43.6s + 1.928}. \tag{20}$$

–The $PI^{\lambda}D^{\delta}$-PSO controller via Oustaloup's approach:

$$C(s) = 11.8738 + \frac{1}{s^{0.733107}} + s^{0.22141}, \tag{21}$$

$$C_{Ous}(s) = \frac{\begin{array}{c}429.5s^{10} + 3.375e004s^9 + 7.778e005s^8 + 6.432e006s^7 + 2.073e007s^6 + 2.652e007s^5 \\ + 1.388e007s^4 + 2.98e006s^3 + 2.688e005s^2 + 9560s + 115\end{array}}{\begin{array}{c}29.26s^{10} + 2402s^9 + 5.664e004s^8 + 4.763e005s^7 + 1.536e006s^6 + 1.933e006s^5 \\ + 9.59e005s^4 + 1.856e005s^3 + 1.377e004s^2 + 364.5s + 2.772\end{array}}, \tag{22}$$

$$H^{PSO}_{Ous}(s) = \frac{\begin{array}{c}61.55s^{10} + 4836s^9 + 1.115e005s^8 + 9.217e005s^7 + 2.971e006s^6 + 3.8e006s^5 \\ + 1.989e006s^4 + 4.27e005s^3 + 3.852e004s^2 + 1370s + 16.48\end{array}}{\begin{array}{c}1.522e-005s^{12} + 0.007604s^{11} + 62.7s^{10} + 4898s^9 + 1.127e005s^8 + 9.318e005s^7 + \\ 3.003e006s^6 + 3.84e006s^5 + 2.009e006s^4 + 4.308e005s^3 + 3.88e004s^2 + 1377s + 16.54\end{array}}. \tag{23}$$

–The $PI^{\lambda}D^{\delta}$-PSO controller via the CFE approach:

$$C(s) = 20.5491 + \frac{1}{s^{0.968724}} + s^{0.091}, \tag{24}$$

$$C_{CFE}(s) = \frac{\begin{array}{c}1.896e004s^{10} + 7.188e005s^9 + 8.023e006s^8 + 3.672e007s^7 + 7.87e007s^6 + 8.372e007s^5 \\ + 4.474e007s^4 + 1.175e007s^3 + 1.431e006s^2 + 7.406e004s + 1335\end{array}}{\begin{array}{c}859.2s^{10} + 3.286e004s^9 + 3.674e005s^8 + 1.678e006s^7 + 3.566e006s^6 + 3.723e006s^5 \\ + 1.913e006s^4 + 4.627e005s^3 + 4.662e004s^2 + 1481s + 1.516\end{array}}, \tag{25}$$

$$H_{CFE}^{PSO}(s) = \frac{\begin{array}{c}2717s^{10}+1.03e005s^9+1.15e006s^8+5.262e006s^7+1.128e007s^6+1.2e007s^5\\+6.411e006s^4+1.684e006s^3+2.05e005s^2+1.061e004s+191.3\end{array}}{\begin{array}{c}0.0004468s^{12}+0.2037s^{11}+2742s^{10}+1.038e005s^9+1.158e006s^8+5.297e006s^7\\+1.135e007s^6+1.207e007s^5+6.451e006s^4+1.693e006s^3+2.06e005s^2+1.064e004s+191.3\end{array}}. \quad (26)$$

–The $PI^{\lambda}D^{\delta}$-BFO controller via 1^{st}-order El-Khazali's approach:

$$C(s) = 8.4891 + \frac{6.0935}{s^{0.7581}} + 20.0919s^{0.8048}, \quad (27)$$

$$C_{\{1^{st}-Kh\}}(s) = \frac{726.4s^2+599.8s+280.1}{5.2s^2+34.65s+6.472}, \quad (28)$$

$$H_{\{1^{st}-Kh\}}^{BFO}(s) = \frac{104.1s^2+85.95s+40.14}{2.704e-006s^4+0.001147s^3+104.2s^2+86.67s+40.27}. \quad (29)$$

–The $PI^{\lambda}D^{\delta}$-BFO controller via 2^{nd}-order El-Khazali's approach:

$$C(s) = 13.8469 + \frac{4.9298}{s^{0.2575}} + 11.8752s^{0.5831}, \quad (30)$$

$$C_{\{2^{nd}-Kh\}}(s) = \frac{96.99s^4+523.9s^3+905.8s^2+503.4s+87.38}{1.252s^4+13.34s^3+30.87s^2+20.18s+3.446}, \quad (31)$$

$$H_{\{2^{nd}-Kh\}}^{BFO}(s) = \frac{13.9s^4+75.07s^3+129.8s^2+72.14s+12.52}{6.51e-007s^6+0.0002788s^5+13.93s^4+75.36s^3+130.4s^2+72.55s+12.59}. \quad (32)$$

–The $PI^{\lambda}D^{\delta}$-BFO controller via Oustaloup's approach:

$$C(s) = 3.2985 + \frac{4.1654}{s^{0.1852}} + 11.3321s^{0.3326}, \quad (33)$$

$$C_{Ous}(s) = \frac{\begin{array}{c}134.9s^{10}+1.05e004s^9+2.631e005s^8+2.325e006s^7+8.435e006s^6+1.197e007s^5\\+7.223e006s^4+1.722e006s^3+1.712e005s^2+6129s+71.8\end{array}}{\begin{array}{c}2.346s^{10}+244.3s^9+7849s^8+8.787e004s^7+3.88e005s^6+6.532e005s^5\\+4.445e005s^4+1.153e005s^3+1.18e004s^2+420.6s+4.626\end{array}}, \quad (34)$$

$$H_{Ous}^{BFO}(s) = \frac{\begin{array}{c}19.33s^{10}+1504s^9+3.77e004s^8+3.332e005s^7+1.209e006s^6+1.715e006s^5\\+1.035e006s^4+2.468e005s^3+2.453e004s^2+878.3s+10.29\end{array}}{\begin{array}{c}1.22e-006s^{12}+0.0006366s^{11}+19.43s^{10}+1511s^9+3.788e004s^8+3.351e005s^7\\+1.217e006s^6+1.729e006s^5+1.044e006s^4+2.492e005s^3+2.477e004s^2+886.9s+10.38\end{array}}. \quad (35)$$

–The $PI^{\lambda}D^{\delta}$-BFO controller via the CFE approach:

$$C(s) = 9.7776 + \frac{14.5668}{s^{0.8676}} + 10.6973s^{0.9061}, \quad (36)$$

$$C_{CFE}(s) = \frac{\begin{array}{c}3.533e005s^{10}+8.136e006s^9+6.829e007s^8+2.69e008s^7+5.908e008s^6+7.955e008s^5\\+6.726e008s^4+3.363e008s^3+8.997e007s^2+1.098e007s+4.815e005\end{array}}{\begin{array}{c}142.9s^{10}+4.654e004s^9+9.041e005s^8+6.302e006s^7+1.902e007s^6+2.757e007s^5\\+1.955e007s^4+6.672e006s^3+9.913e005s^2+5.347e004s+230.1\end{array}}, \quad (37)$$

$$H_{CFE}^{BFO}(s) = \frac{5.063e004s^{10}+1.166e006s^{9}+9.786e006s^{8}+3.854e007s^{7}+8.465e007s^{6}+1.14e008s^{5} +9.639e007s^{4}+4.819e007s^{3}+1.289e007s^{2}+1.573e006s+6.9e004}{7.433e-005s^{12}+0.05525s^{11}+5.065e004s^{10}+1.167e006s^{9}+9.806e006s^{8}+3.868e007s^{7} +8.505e007s^{6}+1.146e008s^{5}+9.679e007s^{4}+4.833e007s^{3}+1.291e007s^{2}+1.574e006s+6.9e004}. \quad (38)$$

To spotlight the dissimilarities between all previous design methods, some numerical results of the closed-loop transfer functions given in (17), (20),(23), (26), (29), (32),(35), and (38) are exhibited in Figure 4, Figure 5, and Table 1.

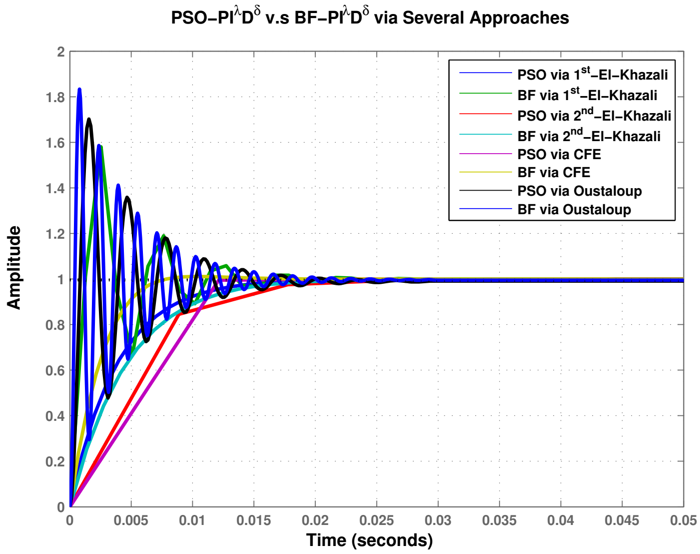

Fig. 4: Step responses of (17), (20),(23), (26) & (29), (32),(35), (38).

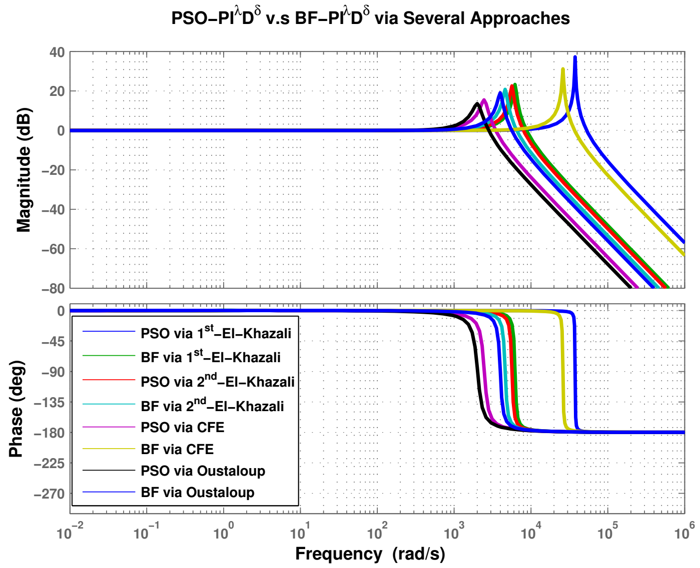

Fig. 5: Bode diagrams of (17), (20),(23), (26) & (29), (32),(35), (38).

A closer examination to the above numerical results demonstrates to us that all proposed controllers are often competing in providing high performance response specifications of all their corresponding closed-loop systems. In particular, there are some slight improvements of the step responses achieved using PSO algorithm over that of BFO algorithm. For example, one can observe that the minimum overshoot of the linear BLDC motor system has been occurred when the $PI^{\lambda}D^{\delta}$-controller is designed by carrying out the PSO algorithm via Oustaloup's approach. Generally,

Table 1: Step responses of (17), (20),(23), (26) & (29), (32),(35), (38)

Step Response	$H^{PSO}_{\{1^{st}-Kh\}}$	$H^{PSO}_{\{2^{nd}-Kh\}}$	H^{PSO}_{CFE}	H^{PSO}_{Ous}	$H^{BFO}_{\{1^{st}-Kh\}}$	$H^{BFO}_{\{2^{nd}-Kh\}}$	H^{BFO}_{CFE}	H^{BFO}_{Ous}
Rise Time	0.0084	0.0114	5.6222e-004	0.0098	0.0010	0.0097	0.0045	2.7177e-004
Settling Time	0.0146	0.0190	0.0192	0.0119	0.0156	0.0161	0.0067	0.0183
Settling Min.	0.9022	0.9754	0.4776	0.9934	0.6642	0.9138	0.9125	0.2946
Settling Max.	0.9998	0.9986	1.7023	0.9997	1.5802	0.9979	1.0110	1.8335
Overshoot	0.3497	0.0465	70.8166	0.0000	58.5431	0.3507	1.1086	85.0407
Peak	0.9998	0.9986	1.7023	0.9997	1.5802	0.9979	1.0110	1.8335
Peak Time	0.0441	0.0533	0.0016	0.0243	0.0025	0.0344	0.0100	7.8800e-004

all feedback design methods satisfy excellent results, except two methods ($PI^{\lambda}D^{\delta}$- PSO via CFE and $PI^{\lambda}D^{\delta}$-BFO via 1^{st}-order El-Khazali's approach) due to the have provided high overshoots as one could observe.

5.2 Design of $PI^{\lambda}D^{\delta}$-controller for Servo DC motor

Many modern industrial applications rely on Servo DC motors in their running. For example, but not limited to, these motors are employed in robotics, especially in regard to determine their precision positioning, and also control their speed. In other words, the Servo DC motors typically use a feedback controller for the purpose of controlling their position and/or their speed. In [25], a Servo motor system has been recently handled in term of enhancing its performance through using Carlson's approach and the 2^{nd}-order El-Khazali's approach. However, likewise to the previous subsection, we purpose, in this part, to design several feedback methods for controlling the position of the Servo DC motor. In [2], in light of its position, LTI system of the Servo DC motor model have been addressed, and then the transfer function of the angular position $\theta(t)$ to the applied voltage $v(t)$ has been obtained. That is;

$$G(s) = \frac{\Theta(s)}{V(s)} = \frac{1.91}{s^3+21s^2+20s}, \tag{39}$$

where $\Theta(s) = \mathscr{L}\{\theta(t)\}$ and $V(s) = \mathscr{L}\{v(t)\}$ are the Laplace transforms of $\theta(t)$ and $v(t)$, respectively. From now on, all $PI^{\lambda}D^{\delta}$-controllers will be tuned optimally by the PSO and BFO algorithms via the four approaches mentioned before in order to examine and compare all dynamic responses for all resultant closed-loop systems. The maximum number of iterations and the population size have been assumed 100 and 20 in both algorithms, respectively. However, the overall results of these two optimizations can be arranged in the following manner.

–The $PI^{\lambda}D^{\delta}$-PSO controller via 1^{st}-order El-Khazali's approach:

$$C(s) = 34.4612 + \frac{57}{s^{0.33223}} + 26.8735s^{0.876195}, \tag{40}$$

$$C_{\{1^{st}-Kh\}}(s) = \frac{592.8s^2+1650s+1390}{1.729s^2+18.72s+10.25}, \tag{41}$$

$$H^{PSO}_{\{1^{st}-Kh\}}(s) = \frac{1132s^2+3151s+2655}{1.729s^5+55.03s^4+438s^3+1722s^2+3356s+2655}. \tag{42}$$

–The $PI^{\lambda}D^{\delta}$-PSO controller via 2^{nd}-order El-Khazali's approach:

$$C(s) = 1 + \frac{49.421}{s^{0.306845}} + 45s^{0.911}, \tag{43}$$

$$C_{\{2^{nd}-Kh\}}(s) = \frac{394.3s^4+1535s^3+2410s^2+1651s+435.8}{0.2231s^4+10.17s^3+29.69s^2+23.22s+4.048}, \tag{44}$$

$$H^{PSO}_{\{2^{nd}-Kh\}}(s) = \frac{753s^4+2931s^3+4603s^2+3154s+832.4}{0.2231s^7+14.85s^6+247.7s^5+1603s^4+4017s^3+5153s^2+3235s+832.4}. \tag{45}$$

–The $PI^{\lambda}D^{\delta}$-PSO controller via Oustaloup's approach:

$$C(s) = 59 + \frac{1}{s^{0.165}} + 12.6794s^{0.387156}, \tag{46}$$

$$C_{Ous}(s) = \frac{288.4s^{10} + 2.566e004s^9 + 7.358e005s^8 + 7.561e006s^7 + 3.156e007s^6 + 5.131e007s^5 + 3.437e007s^4 + 8.905e006s^3 + 9.201e005s^2 + 3.343e004s + 376.3}{2.138s^{10} + 231.3s^9 + 7688s^8 + 8.918e004s^7 + 4.073e005s^6 + 7.101e005s^5 \; 4.997e005s^4 + 1.342e005s^3 + 1.42e004s^2 + 524.4s + 5.947}, \tag{47}$$

$$H^{PSO}_{Ous}(s) = \frac{550.8s^{10} + 4.901e004s^9 + 1.405e006s^8 + 1.444e007s^7 + 6.028e007s^6 + 9.8e007s^5 + 6.565e007s^4 + 1.701e007s^3 + 1.757e006s^2 + 6.386e004s + 718.7}{2.138s^{13} + 276.2s^{12} + 1.259e004s^{11} + 2.558e005s^{10} + 2.483e006s^9 + 1.245e007s^8 + 3.8e007s^7 + 8.511e007s^6 + 1.108e008s^5 + 6.864e007s^4 + 1.73e007s^3 + 1.768e006s^2 + 6.397e004s + 718.7}. \tag{48}$$

–The $PI^{\lambda}D^{\delta}$-PSO controller via the CFE approach:

$$C(s) = 48 + \frac{1}{s^{0.177}} + 25.1508s^{0.166}, \tag{49}$$

$$C_{CFE}(s) = \frac{230.6s^{10} + 1.064e004s^9 + 1.621e005s^8 + 9.656e005s^7 + 2.664e006s^6 + 3.606e006s^5 + 2.453e006s^4 + 8.146e005s^3 + 1.238e005s^2 + 7134s + 132.8}{2.254s^{10} + 116s^9 + 1910s^8 + 1.202e004s^7 + 3.468e004s^6 + 4.881e004s^5 + 3.441e004s^4 + 1.183e004s^3 + 1862s^2 + 111.8s + 2.142}, \tag{50}$$

$$H^{PSO}_{CFE}(s) = \frac{440.5s^{10} + 2.031e004s^9 + 3.097e005s^8 + 1.844e006s^7 + 5.088e006s^6 + 6.888e006s^5 + 4.686e006s^4 + 1.556e006s^3 + 2.365e005s^2 + 1.363e004s + 253.6}{2.254s^{13} + 163.3s^{12} + 4391s^{11} + 5.488e004s^{10} + 3.456e005s^9 + 1.327e006s^8 + 3.597e006s^7 + 6.799e006s^6 + 7.826e006s^5 + 4.962e006s^4 + 1.596e006s^3 + 2.388e005s^2 + 1.367e004s + 253.6}. \tag{51}$$

–The $PI^{\lambda}D^{\delta}$-BFO controller via 1^{st}-order El-Khazali's approach:

$$C(s) = 20.2744 + \frac{15.5467}{s^{0.2245}} + 18.3304s^{0.4752}, \tag{52}$$

$$C_{\{1^{st}-Kh\}}(s) = \frac{104.7s^2 + 212.8s + 115.7}{1.434s^2 + 4.28s + 2.287}, \tag{53}$$

$$H^{BFO}_{\{1^{st}-Kh\}}(s) = \frac{200s^2 + 406.5s + 221}{1.434s^5 + 34.39s^4 + 120.8s^3 + 333.7s^2 + 452.2s + 221}. \tag{54}$$

–The $PI^{\lambda}D^{\delta}$-BFO controller via 2^{nd}-order El-Khazali's approach:

$$C(s) = 21.1803 + \frac{16.0728}{s^{0.9151}} + 17.0010s^{0.5781}, \tag{55}$$

$$C_{\{2^{nd}-Kh\}}(s) = \frac{230.4s^4 + 980.2s^3 + 1386s^2 + 792.7s + 180.5}{2.147s^4 + 20.17s^3 + 30.7s^2 + 12.51s + 0.2649}, \tag{56}$$

$$H^{BFO}_{\{2^{nd}-Kh\}}(s) = \frac{440s^4 + 1872s^3 + 2647s^2 + 1514s + 344.7}{2.147s^7 + 65.26s^6 + 497.2s^5 + 1501s^4 + 2749s^3 + 2902s^2 + 1519s + 344.7}. \tag{57}$$

–The $PI^{\lambda}D^{\delta}$-BFO controller via Oustaloup's approach:

$$C(s) = 5.9725 + \frac{19.2767}{s^{0.1901}} + 7.3436s^{0.3402}, \tag{58}$$

$$C_{Ous}(s) = \frac{\begin{array}{c}118.1s^{10} + 1.01e004s^9 + 2.858e005s^8 + 2.932e006s^7 + 1.259e007s^6 + 2.138e007s^5 \\ + 1.54e007s^4 + 4.323e006s^3 + 4.955e005s^2 + 1.996e004s + 257.6\end{array}}{\begin{array}{c}2.4s^{10} + 250.6s^9 + 8058s^8 + 9.036e004s^7 + 3.995e005s^6 + 6.734e005s^5 \\ + 4.587e005s^4 + 1.192e005s^3 + 1.22e004s^2 + 435.7s + 4.791\end{array}}, \tag{59}$$

$$H_{Ous}^{BFO}(s) = \frac{\begin{array}{c}225.5s^{10} + 1.93e004s^9 + 5.459e005s^8 + 5.599e006s^7 + 2.405e007s^6 + 4.083e007s^5 \\ + 2.941e007s^4 + 8.256e006s^3 + 9.463e005s^2 + 3.812e004s + 492\end{array}}{\begin{array}{c}2.4s^{13} + 301s^{12} + 1.337e004s^{11} + 2.648e005s^{10} + 2.477e006s^9 + 1.142e007s^8 + 2.819e007s^7 \\ + 4.727e007s^6 + 5.252e007s^5 + 3.205e007s^4 + 8.51e006s^3 + 9.551e005s^2 + 3.822e004s + 492\end{array}}. \tag{60}$$

–The $PI^{\lambda}D^{\delta}$-BFO controller via the CFE approach:

$$C(s) = 20.8307 + \frac{15.1690}{s^{0.8666}} + 20.5882s^{0.9161}, \tag{61}$$

$$C_{CFE}(s) = \frac{\begin{array}{c}8.585e005s^{10} + 1.971e007s^9 + 1.643e008s^8 + 6.348e008s^7 + 1.322e009s^6 + 1.616e009s^5 \\ + 1.203e009s^4 + 5.336e008s^3 + 1.302e008s^2 + 1.502e007s + 6.356e005\end{array}}{\begin{array}{c}158.2s^{10} + 5.684e004s^9 + 1.108e006s^8 + 7.74e006s^7 + 2.338e007s^6 + 3.389e007s^5 \\ + 2.403e007s^4 + 8.195e006s^3 + 1.216e006s^2 + 6.533e004s + 262.6\end{array}}, \tag{62}$$

$$H_{CFE}^{BFO}(s) = \frac{\begin{array}{c}1.64e006s^{10} + 3.764e007s^9 + 3.139e008s^8 + 1.213e009s^7 + 2.526e009s^6 + 3.086e009s^5 \\ + 2.298e009s^4 + 1.019e009s^3 + 2.487e008s^2 + 2.868e007s + 1.214e006\end{array}}{\begin{array}{c}158.2s^{13} + 6.017e004s^{12} + 2.305e006s^{11} + 3.38e007s^{10} + 2.457e008s^9 + 9.935e008s^8 + 2.416e009s^7 \\ + 3.717e009s^6 + 3.74e009s^5 + 2.488e009s^4 + 1.045e009s^3 + 2.5e008s^2 + 2.868e007s + 1.214e006\end{array}}. \tag{63}$$

For more insight, Figure 6, Figure 7, and Table 2 highlight the similarities and dissimilarities aspects between all previous design methods.

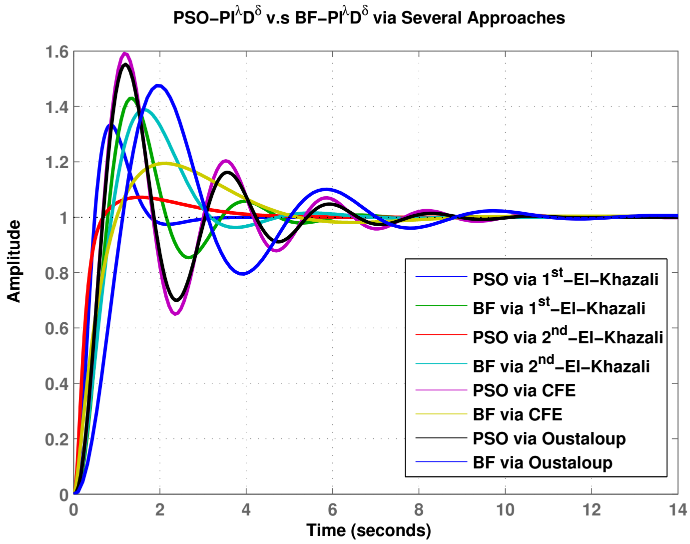

Fig. 6: Step responses of (42), (45),(48), (51) & (54), (57),(60), (63).

Table 2: Step responses of (42), (45),(48), (51) & (54), (57),(60), (63)

Step Response	$H^{PSO}_{\{1^{st}-Kh\}}$	$H^{PSO}_{\{2^{nd}-Kh\}}$	H^{PSO}_{CFE}	H^{PSO}_{Ous}	$H^{BFO}_{\{1^{st}-Kh\}}$	$H^{BFO}_{\{2^{nd}-Kh\}}$	H^{BFO}_{CFE}	H^{BFO}_{Ous}
Rise Time	0.3160	0.3885	0.4279	0.4368	0.5067	0.5867	0.7086	0.7415
Settling Time	2.4807	3.4491	8.3970	7.3866	5.4051	4.3023	4.7133	10.0759
Settling Min.	0.9367	0.9044	0.6498	0.7000	0.8539	0.9033	0.9053	0.7949
Settling Max.	1.3333	1.0719	1.5909	1.5519	1.4290	1.3883	1.1942	1.4751
Overshoot	33.3316	7.1945	59.0943	55.1936	42.8986	38.8303	19.4189	47.5088
Peak	1.3333	1.0719	1.5909	1.5519	1.4290	1.3883	1.1942	1.4751
Peak Time	0.8599	1.5389	1.1751	1.2024	1.3631	1.6305	2.1162	1.9211

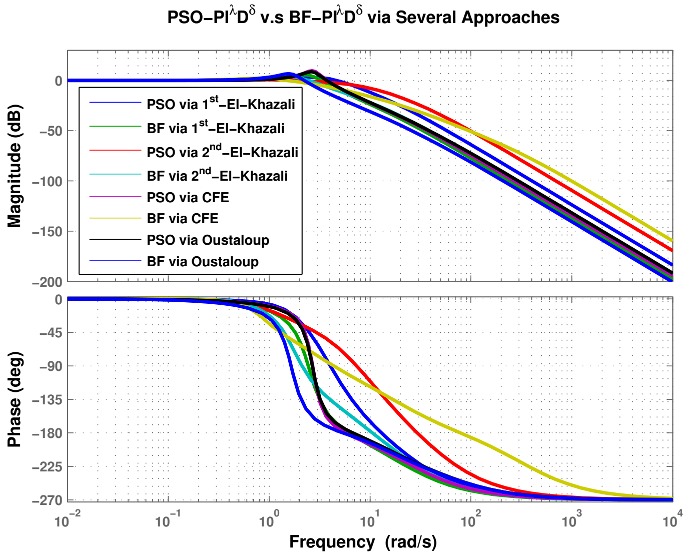

Fig. 7: Bode diagrams of (42), (45),(48), (51) & (54), (57),(60), (63).

In view of the above numerical results, another fiercely competition can be clearly observed between all the proposed controllers. Here, the PSO algorithm via the four considered approaches mostly shows significant improvements in the step response characteristics over that of BFO algorithm. More particulary, we find that when the $PI^{\lambda}D^{\delta}$-controller is designed using the PSO algorithm via the 2^{nd}-order El-Khazali's approach, the minimum overshoot of the Servo DC motor system has been occurred; whereas the fast rise time and fast settling time have been achieved, when such controller has been designed using the PSO algorithm via the 1^{st}-order El-Khazali's approach.

6 Conclusion

Several feedback control methods have been designed for two industrial applications; the Brushless DC motor and the Servo DC motor. The purpose of all these methods is to find an optimal $PI^{\lambda}D^{\delta}$-controller that provides the closed-loop system with the best dynamic response. In order to achieve this goal, two algorithms, Particle Swarm Optimization (PSO) and Bacteria Foraging Optimization (BFO), have been successfully carried out along with the use of four approaches of the fractional-order integro-differential Laplacian operators $s^{\pm\alpha}$, where $0 < \alpha < 1$. Those approaches are: The Continued Fractional Expansion (CFE), Oustaloup's, the 1^{st}- and the 2^{nd}-order El-Khazali's approach. It can be inferred, in the light of the obtained numerical results, that all proposed controllers have fiercely competed in providing high performance response specifications of all their corresponding closed-loop systems. In addition, the PSO algorithm along with all four considered approaches, especially via Oustaloup's as well as the 1^{st}- and the 2^{nd}-order El-Khazali's approaches, have shown mostly significant improvements in the characteristics of the step response over that of what the BFO algorithm have shown.

Acknowledgments

The first author thanks the kind hospitality of the College of Humanities and Sciences of Ajman University during his sabbatical leave and thanks the University of Jordan which financially supported him to leave for sabbatical.

References

[1] M. Khanra, J. Pal and K. Biswas, Rational approximation of fractional operator — A comparative study, *2010 Int. Conf. Pow. Cont. Emb. Sys.*, 1–5, Allahabad, India, 29 Nov.-1 Dec. 2010.
[2] P. Kumar, S. Chatterjee, D. Shah, U. K. Saha and S. Chatterjee, On comparison of tuning method of FOPID controller for controlling field controlled DC Servo motor, *Cog. Engin.* **4**, (2017).
[3] I. Podlubny, Fractional-order systems and $PI^{\lambda}D^{\mu}$-controllers, *IEEE Transac. Auto. Cont.* **44**, 208—214 (1999).
[4] W. Lin and Z. Chongquan, Design of optimal fractional-order PID controllers using particle swarm optimization algorithm for DC motor system, *2015 IEEE Adv. Inf. Tech. Elect. Auto. Cont. Conf. (IAEAC)*, 175–179, Chongqing, China, Dec. 2015.
[5] K. E. Dagher, Design of an auto-tuning PID controller for systems based on slice genetic algorithm, *Iraqi J. Comp. Commun. Cont. Sys. Engin.* **13**, (2013).
[6] S. Das, A. Biswas, S. Dasgupta and A. Abraham, Bacterial foraging optimization algorithm: Theoretical foundations, analysis, and applications, in A. Abraham, A.E. Hassanien, P. Siarry, A. Engelbrech, (eds.): *Foundations of Computational Intelligence Volume 3. Studies in Computational Intelligence*, Springer, Berlin, Heidelberg, 2009.
[7] J. Kennedy and R. Eberhart, Particle swarm optimization, *Proc. ICNN'95 - Int. Conf. Neu. Net.*, 1942–1948, Perth, WA, Australia, 27 Nov.-1 Dec. 1995.
[8] M. Nasri, H. Nezamabadi-pour and M. Maghfoori, A PSO-based optimum design of PID controller for a linear brushless DC motor, *Proc. World Aca. Sci. Engin. Tech. Vol. 20*, 211–215, ISCA, USA, April 2007.
[9] K. M. Passino, Distributed optimization and control using only a germ of intelligence, *The 2000 IEEE Int. Symp. Intel. Cont. Held jointly with the 8th IEEE Mediter. Conf. Cont. Auto. (Cat. No.00CH37147)*, 5–13, Rio Patras, Greece, July 2000.
[10] S. Momani, R. El-Khazali and I. M. Batiha, Tuning PID and $PI^{\lambda}D^{\delta}$ controllers using particle swarm optimization algorithm via El-Khazali's approach, *AIP Confer. Proc.* **2172**, (2019).
[11] B. D. Halilu, E. C. Anene, E. E. Omigzegba, L. Maijama'a and S. A. Baraza, Optimization of PID controller gains for identified magnetic levitation plant using bacteria foraging algorithm, *Int. J. Eng. Mod. Tech.* **5**, 12–18 (2019).
[12] M. A. Muñoz, S. K. Halgamuge, W. Alfonso and E. F. Caicedo, Simplifying the bacteria foraging optimization algorithm, *IEEE Cong. Evolut. Comput.*, 1–7, Barcelona, Spain, July 2010.
[13] S. Momani, I. M. Batiha and R. El-Khazali, Design of $PI^{\lambda}D^{\delta}$-heart rate controllers for cardiac pacemaker, *2019 IEEE Int. Symp. Sig. Pro. Infor. Tech. (ISSPIT)*, 1–5, Ajman, United Arab Emirates, Dec. 2019.
[14] I. M. Batiha, R. El-Khazali and S. Momani, Dynamic responses of PI^{λ}, PD^{δ}, and $PI^{\lambda}D^{\delta}$ controllers for prosthetic hand model using PSO algorithm, *2019 IEEE Int. Symp. Sig. Pro. Infor. Tech. (ISSPIT)*, 1–6, Ajman, United Arab Emirates, Dec. 2019.
[15] A. Kh. Gil'mutdinov, P. A. Ushakov and R. El-Khazali, *Fractal elements and their applications*, Springer International Publishing, Switzerland, 2017.
[16] R. El-Khazali, I. M. Batiha and S. Momani, Approximation of fractional-order operators, in P. Agarwal, D. Baleanu, Y. Chen, S. Momani, J. Machado, (eds.): *Fractional Calculus. ICFDA 2018. Springer Proceedings in Mathematics & Statistics, vol 303*, Springer, Singapore, 121–151 (2019).
[17] H. Ramezanian and S. Balochian, Optimal design a fractional-order PID controller using particle swarm optimization algorithm, *Int. J. Cont. Auto.* **6**, 55—56 (2013).
[18] R. El-Khazali, Fractional-order $LC^{\alpha}L$ filter-based grid connected PV systems, *2019 IEEE 62nd Int. Midwest Symp. Cir. Sys. (MWSCAS)*, 533–536, Dallas, TX, USA, Aug. 2019.
[19] R. El-Khazali, Fractional-order $PI^{\lambda}D^{\mu}$ controller design, *Comp. and Math. with App.* **66**, 639–646 (2013).
[20] I. M. Batiha, R. El-Khazali, A. Alsaedi and S. Momani, The general solution of singular fractional-order linear time-invariant continuous systems with regular pencils, *Entropy* **20**, (2018).
[21] A. Tepljakov, *Fractional-order modeling and control of dynamic systems*, Ph.D thesis, Tallin University of Technology, Tallinn, 2015.
[22] I. M. Batiha, *Optimal design and tuning of fractional-order $PI^{\lambda}D^{\delta}$ controllers using particle swarm optimization techneque*, Ph.D thesis, The University of Jordan, Amman, 2018.
[23] I. Podlubny, L. Dorcak and I. Kostial, On fractional derivatives, fractional-order dynamic systems and $PI^{\lambda}D^{\mu}$ -controllers, *Proc. 36th IEEE Conf. Dec. Cont.*, 4985–4990, San Diego, CA, USA, Dec. 1997.
[24] A. Biswas, S. Dasgupta, S. Das and A. Abraham, Synergy of PSO and bacterial foraging optimization – A Comparative study on numerical benchmarks, in E. Corchado, J.M. Corchado, A. Abraham, (eds.): *Innovations in Hybrid Intelligent Systems. Advances in Soft Computing, vol 44*, Springer, Berlin, Heidelberg, 255–263 (2007).
[25] R. El-Khazali, On the biquadratic approximation of fractional-order Laplacian operators, *Analog Int. Circ. Sig. Proc.* **82**, 503–517 (2015).

[26] A. Oustaloup, F. Levron, B. Mathieu and F. M. Nanot, Frequency band complex noninteger differentiator: characterization and synthesis, *IEEE Transac. Circ. Sys. I: Fun. Theo. App.* **47**, 25–39 (2000).
[27] B. T. Krishna, Studies on fractional order differentiators and integrators: A survey, *Sig. Pro.* **91**, 386—426 (2011).
[28] Priyanka and M. S. Aspalli, Speed control of BLDC motor using PID controller and genetic algorithm, *Speed Cont. BLDC Motor PID Controller Gene. Algo.* **6**, 3601—3605 (2017).
[29] R. Bindu and M. K. Namboothiripad, Tuning of PID controller for DC Servo motor using genetic algorithm, *Int. J. Emer. Tech. Adv. Eng.* **2**, 310–314 (2012).
[30] M. Umar, F. Amin, H. Abdul Wahab and D. Baleanu, Unsupervised constrained neural network modeling of boundary value corneal model for eye surgery, *App. Soft Comput.* **85**, (2019).
[31] B. Farnad, A. Jafarian and D. Baleanu, A new hybrid algorithm for continuous optimization problem, *App. Math. Model.* **55**, 652–673 (2018).
[32] M. R. Faieghi, H. Delavari and D. Baleanu, A novel adaptive controller for two-degree of freedom polar robot with unknown perturbations, *Commun. Nonlin. Sci. Numer. Sim.* **17**, 1021–1030 (2012).